

Lattice deformation in epitaxial Fe_3O_4 films on MgO substrates studied by polarized Raman spectroscopy

Yang Yang(杨洋), Qiang Zhang(张强), Wenbo Mi(米文博), Xixiang Zhang(张西祥)

Citation: Chin. Phys. B . 2020, 29(8): 083302 . **doi:** 10.1088/1674-1056/ab9615
Journal homepage: http://cpb.iphy.ac.cn; http://iopscience.iop.org/cpb

What follows is a list of articles you may be interested in

Photoassociation spectra of ultracold $^{85}Rb_2$ molecule in 0_u^+ long range state near the $5S_{1/2}+5P_{1/2}$ asymptote

Guodong Zhao(赵国栋), Dianqiang Su(苏殿强), Zhonghua Ji(姬中华), Tengfei Meng(孟腾飞), Yanting Zhao(赵延霆), Liantuan Xiao(肖连团), Suotang Jia(贾锁堂)

Chin. Phys. B . 2017, 26(8): 083301 . **doi:** 10.1088/1674-1056/26/8/083301

High-resolution photoassociation spectroscopy of ultracold Cs_2 long-range 0_g^- state：The external well potential depth

Liu Wen-Liang, Wu Ji-Zhou, Ma Jie, Xiao Lian-Tuan, Jia Suo-Tang

Chin. Phys. B . 2014, 23(1): 013301 . **doi:** 10.1088/1674-1056/23/1/013301

High resolution photoassociation spectra of an ultracold Cs_2 long-range 0_u^+ ($6S_{1/2}+6P_{1/2}$) state

Chen Peng, Li Yu-Qing, Zhang Yi-Chi, Wu Ji-Zhou, Ma Jie, Xiao Lian-Tuan, Jia Suo-Tang

Chin. Phys. B . 2013, 22(9): 093301 . **doi:** 10.1088/1674-1056/22/9/093301

Reanalysis of the photoassociation spectrum of $^{133}Cs_2$ ($6P_{3/2}$) 1_g state

Ma Jie, Li Yu-Qing, Wu Ji-Zhou, Fan Qun-Chao, Feng Hao, Sun Wei-Guo, Xiao Lian-Tuan, Jia Suo-Tang

Chin. Phys. B . 2013, 22(8): 083302 . **doi:** 10.1088/1674-1056/22/8/083302

Stabilizing photoassociated Cs_2 molecules by optimal control

Zhang Wei, Xie Ting, Huang Yin, Wang Gao-Ren, Cong Shu-Lin

Chin. Phys. B . 2013, 22(1): 013301 . **doi:** 10.1088/1674-1056/22/1/013301

Enhancement of the photoassociation of ultracold atoms via a non-resonant magnetic field*

Ji-Zhou Wu(武寄洲)[1,2], Yu-Qing Li(李玉清)[1,2,†], Wen-Liang Liu(刘文良)[1,2], Peng Li(李鹏)[3], Xiao-Feng Wang(王晓锋)[1], Peng Chen(陈鹏)[1], Jie Ma(马杰)[1,2,3], Lian-Tuan Xiao(肖连团)[1,2], and Suo-Tang Jia(贾锁堂)[1,2]

[1] *State Key Laboratory of Quantum Optics and Quantum Optics Devices, Institute of Laser Spectroscopy, Shanxi University, Taiyuan* 030006, *China*
[2] *Collaborative Innovation Center of Extreme Optics, Shanxi University, Taiyuan* 030006, *China*
[3] *College of Physics and Electronics Engineering, Shanxi University,Taiyuan* 030006, *China*

(Received 20 April 2020; revised manuscript received 15 May 2020; accepted manuscript online 25 May 2020)

We report an effective method for enhancing the photoassociation of ultracold atoms using a non-resonant magnetic field, which enables the manipulation of the coupling between the wavefunctions of the colliding atomic pairs and the excited molecules. A series of photoassociation spectra are measured for different magnetic fields. We show that the photoassociation rate is significantly dependent on the non-resonant magnetic field. A qualitatively theoretical explanation is provided, and shows a good agreement with the experimental result.

Keywords: photoassociation, ultracold atoms, magnetic field

PACS: 33.20.Sn, 34.50.−s **DOI:** 10.1088/1674-1056/ab9611

1. Introduction

Investigations on ultracold molecules have led to significant progresses in precision measurement,[1] quantum computation,[2] quantum simulation,[3] and the control of ultracold chemical reactions.[4] Among various approaches proposed for producing ultracold molecules, the photoassociation (PA) of ultracold atoms, in which two colliding atoms resonantly absorb a photon to form an excited molecule,[5] has been shown to be one of the most efficient and standard techniques to obtain molecules at microkelvin or even nanokelvin temperatures.[6] Moreover, PA is also widely applied in realizing optical Feshbach resonance (FR) for the effective control of the interaction of two colliding ultracold atoms, which is particularly useful for alkaline-earth systems with no hyperfine structures in their ground states.[7,8] Recently, PA is used to produce the long-range, homonuclear Rydberg molecules,[9] whose internuclear separations extend to several thousands of a_0 (Bohr radius).

In many contexts, the PA rate is mainly determined by the wavefunction coupling between the colliding ground state atomic pairs and the excited state molecules,[10] and plays an important role in PA and related experiments. A higher PA rate can increase the production of ultracold molecules with considerable yields. Nevertheless, the PA rate is limited by the low density of ultracold atomic pairs at the short internuclear distances. Over the past decade, many theoretical schemes have been proposed for enhancing PA, such as increasing the atomic pairs density within the PA window by accelerating the velocity of atoms,[11] shaping the PA laser pulse by using a controlled frequency chirp,[12] and introducing a static electric field on the PA.[13] However, none of these studies are currently feasible in experiment. It should be noted that a FR-optimized PA has been proposed theoretically[14] and realized experimentally for enhancing PA.[15,16] Recently, benefiting from the high PA rate, FR-optimized PA is also used to measure vibrational levels lower than those accessible using traditional PA spectroscopy[17] and to effectively control atom–molecule conversion using ultranarrow PA transitions.[18] So far, the effect of the magnetic field[19,20] that is far away from the Feshbach Resonance on the PA has not yet been fully investigated.

In this paper, we report on the enhanced PA of ultracold Cs atoms in a crossed optical dipole trap, in which the PA rate coefficient is greatly increased by utilizing a non-resonant external magnetic field. Our research is a good extension to the technique of FR-optimized PA, where the magnetic field alters the wavefunction of the colliding atoms. In our scheme, the PA rate coefficient presents a monotonously continuous dependence on the increasing magnetic field, corresponding to the growth of the atomic scattering length.[21] A simple theoretical model is provided to explain the experimental results. Our observation of enhanced PA opens up the possibility of

*Project supported by the National Key Research and Development Program of China (Grant No. 2017YFA0304203), the National Natural Science Foundation of China (Grant Nos. 61722507, 61675121, and 61705123), PCSIRT, China (Grant No. IRT17R70), 111 Project, China (Grant No. D18001), the Program for the Outstanding Innovative Teams of Higher Learning Institutions of Shanxi (OIT), China, the Applied Basic Research Project of Shanxi Province, China (Grant Nos. 201801D221004, 201901D211191, and 201901D211188), the Shanxi 1331 KSC, and Collaborative Grant by the Russian Foundation for Basic Research and the National Natural Science Foundation of China (Grant Nos. 6191101339 and 20-53-53025 in the RFBR classification).

†Corresponding author. E-mail: lyqing2006@sxu.edu.cn

© 2020 Chinese Physical Society and IOP Publishing Ltd

controlling atom–molecule conversion using a non-resonant external magnetic field without the large three-body loss of atoms near FR.

2. Experiment

We start with ultracold Cs atoms in a vapor loaded magneto-optical trap (MOT) at a background pressure of 3×10^{-8} Pa, the experimental setup is shown in Fig. 1(a). Following the compressed MOT and optical molasses, 3×10^{7} atoms are obtained with a peak density of $\sim10^{11}$ cm^{-3}. Then, the atoms are transferred to a three-dimensional optical lattice, and degenerated Raman sideband cooling is applied to cool the atoms to a low temperature of ~1.7 μK and to polarize them in the desired $F=3$, $m_F=3$ state. A far-off resonance optical dipole trap, which consists of two crossing laser beams with an angle of 90°, is employed to load the atoms.[22,23] The powers of the two laser beams of the crossed dipole trap are 7.0 W and 7.2 W with beam waists of 230 μm and 240 μm at the trap center, respectively. The number of atoms is measured using an absorption image technique.

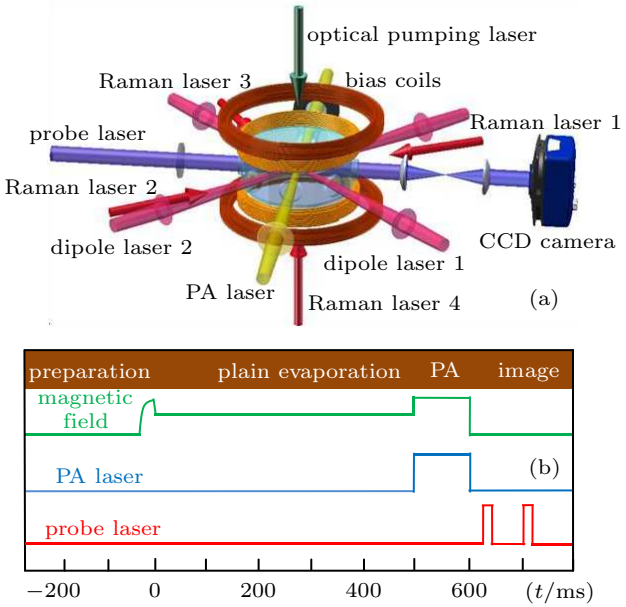


Fig. 1. (a) Experimental setup. Raman lasers 1–4 and an optical pumping laser are applied to implement the Raman sideband cooling. Dipole lasers 1 and 2 are applied to construct the crossed dipole trap. Bias coils are used to produce the external magnetic field. The probe laser passes through the trapped atoms, and the number and density of atoms are measured using the absorption image technique. (b) Experimental sequence for manipulation of the magnetic field, PA laser, and probe laser of absorption image.

Figure 1(b) shows the experimental sequence. In order to eliminate the large three-body loss, the plain evaporation is implemented at the magnetic field of $B=75$ G for 500 ms, where the scattering length of cold atoms is about 1200 a_0[24] with a large three-body loss. Then the magnetic field is tuned to the value of interest. PA is performed by illuminating the atomic sample using a PA laser for 100 ms. A widely tuneable Ti: sapphire laser system (Coherent MBR-110, power ~1 W, linewidth ~0.1 MHz) serves as the PA laser, with a beam waist of ~150 μm and an intensity of ~125 W/cm^2. The frequency of the PA laser is tuned to the vicinity of the resonant transition from the atomic ground state to the molecular excited state of the vibrational level $v=10$ of the pure long-range 0_g^- state (corresponding to a wavenumber ~11672.05 cm^{-1}) below the Cs_2 $6S_{1/2}+6P_{3/2}$ dissociation limit. The long-time frequency drift of the PA laser is less than 500 kHz by locking to its self-reference cavity. The absolute laser frequency is measured using a high-precision wavelength meter, which is repeatedly calibrated against the Cs atomic hyperfine resonant transition.[25] When the frequency of the PA laser is resonant with the transition from the ground atoms to excited molecules, it leads to a large loss of atoms. Most of the excited molecules spontaneously decay into pairs of hot atoms that escape the trap, while the rest randomly and spontaneously radiate into a small number of ground molecules. Considering the negligible three-body loss resulting from the reduction of the atomic density during the plain evaporation process, the atom loss is mainly attributed to the inelastic loss induced by PA.

Figure 2(a) shows a typical PA spectrum for the vibrational level $v=10$ of the Cs_2 0_g^- state below the dissociation limit ($6S_{1/2}+6P_{3/2}$). The resolved rotational levels of $J=0$ and $J=2$ are clearly observed. In order to investigate the influence of the external magnetic field on the PA, we have systematically record the PA spectra for $J=2$, $v=10$ at different magnetic fields of 87 G, 96 G, 108 G, and 120 G, at which the number of atoms remaining in the dipole trap after PA are $(1.3\pm0.03)\times10^5$, $(1.01\pm0.05)\times10^5$, $(0.87\pm0.08)\times10^5$, $(0.7\pm0.02)\times10^5$, respectively, as shown in Fig. 2(b). It can be found that the maximum ratio of the atom loss is up to 70%. The Lorentzian fitting is applied to the experimental data.

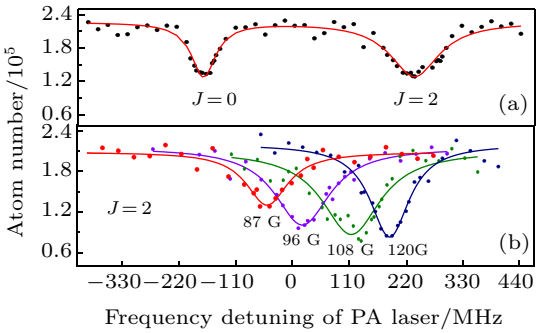


Fig. 2. (a) PA spectrum of the $v=10$ vibrational level of Cs_2 long-range 0_g^- state without the magnetic field. (b) The number of atoms as a function of the frequency detuning of the PA laser with the magnetic fields of 87 G (red dots), 96 G (violet dots), 108 G (green dots), and 120 G (navy dots) for $J=2$. The solid curves are the fittings using a Lorentzian function.

As the magnetic field increases, the number of atoms remaining in the trap after PA gradually decreases. Here we focus on the range of the magnetic field from 85 G to 120 G,

where the Cs atomic s-wave scattering length a monotonically increases with magnetic field B, as shown in Fig. 3(a).[21] It should be noted that there is no FR in this range for Cs atoms in the $F = 3$, $m_F = 3$ state, thus allowing us to investigate the dependence of the PA rate coefficient on the non-resonant magnetic field. In addition, we can also observe the shift of the PA resonance frequency with the magnetic field at the same PA laser intensity, which has been experimentally investigated in our previous work.[26] The influence of the external magnetic field on the PA is mainly attributed to the variation of the coupling between atomic and molecular wavefunctions, where the magnetic field changes the atomic scattering length, leading to the variation of the atomic wavefunction.[16]

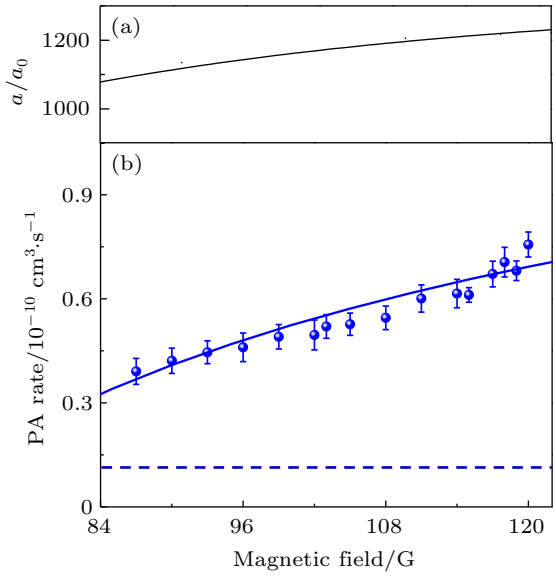


Fig. 3. (a) Theoretical scattering length. (b) PA rate coefficient as a function of magnetic field for rotational level $J = 2$ in $v = 10$. The dots are experimental data. The solid lines are the results of theoretical calculation. The dashed lines show the PA rate coefficient without the magnetic field.

Furthermore, PA rate coefficient $K_{\rm PA}$ is often written as $K_{\rm PA} = (n_0 - n_t)/n_0 n_t t$,[27] where n_0 is the atomic density before switching on the PA laser, n_t is the atom density after switching off the PA laser, t is the PA duration time. The dependence of the PA rate coefficient for $J = 2$ on the magnetic field is shown in Fig. 3(b). The PA rate coefficient is strongly dependent on the external non-resonant magnetic field, and continuously increases with the magnetic field. The observed PA rate coefficient varies from 0.39×10^{-10} cm^3/s to 0.76×10^{-10} cm^3/s when the magnetic field increases from 85 G to 120 G. The errors are mainly from the error in determining the resonance frequency, the fitting error, and the systematic uncertainty which is induced by the fluctuation of the number of trapped atoms in each experimental cycle. Thus the PA of ultracold Cs atoms can be substantially enhanced by using a non-resonant magnetic field.

3. Analysis

A brief qualitative analysis is used to explain the observed results. The PA rate coefficient is determined by the coupling between the s-wave scattering wavefunction of the initially colliding atomic pairs and the wavefunction of the excited molecular level under a PA laser field,[10,14] and can be expressed as

$$K_{\rm PA} = \Gamma \int |\langle \Psi(\upsilon, J)|V_{\rm eg}|\Phi_k\rangle|^2 {\rm d}r, \tag{1}$$

where Γ is a coefficient related to the PA laser intensity and atomic sample temperature, $V_{\rm eg}$ is the dipole moment for the transition between the atomic state $|\Phi_k\rangle$ and the excited molecular state $|\Psi(\upsilon, J)\rangle$, and r is the interatomic distance. For a certain excited molecular level, the PA rate coefficient is mainly determined by the atomic wavefunction Φ_k, which can be described by using a square-well model.[28] Considering the threshold behavior of atomic scattering with the van der Waals interaction, the size of the square-well is chosen to be the mean scattering length $\bar{a}$. The atomic wavefunction is given as

$$\begin{aligned} \Phi_k(r) &= \Phi_{k,r>\bar{a}}(r) + \Phi_{k,r\le\bar{a}}(r) \\ &= \sqrt{\frac{2m_{\rm r}}{\pi\hbar^2 k}} \sin(kr+\eta) + A\sin(k_1 r), \end{aligned} \tag{2}$$

where $\Phi_{k,r>\bar{a}}(r)$ is the wavefunction for $r > \bar{a}$, $k = \sqrt[1/2]{2Em_{\rm r}/\hbar^2}$, $m_{\rm r}$ is the reduced mass, and E is the colliding energy of atoms. The scattering phase shift η can be solved by a precise expression of $\cot\eta = -1/(ak) + r_0 k/2$, where a is the s-wave scattering length and r_0 is the effective range. For $r \le \bar{a}$, $\Phi_{k,r\le\bar{a}}(r) = A\sin(k_1 r)$, where the parameters A and k_1 can be derived using the continuous boundary condition at $r = \bar{a}$. For Cs atoms in the $F = 3$, $m_F = 3$ state, the scattering length is

$$a/a_0 = (1722 + 1.52B)\left(1 - \frac{28.72}{B + 11.74}\right), \tag{3}$$

where B is the magnetic field in units of Gauss.[21] Thus, we can change the scattering length a by using the external non-resonant magnetic field B, then change the atomic wavefunction $\Phi_{k,r>\bar{a}}(r)$. Although the magnetic field only changes the wavefunction $\Phi_{k,r>\bar{a}}(r)$ of the atoms with the interatomic distance $r > \bar{a}$, the continuous boundary condition in the quantum mechanics leads to the variation of the wavefunction of the atoms with the interatomic distance $r \le \bar{a}$, where the PA of colliding atomic pair occurs. As a result, the PA rate coefficient represents the dependence on the magnetic field. The wavefunctions $|\Psi(\upsilon, J)\rangle$ are derived according to the reexamination potential curve for excited Cs molecules.[29] The theoretical PA rate coefficients for the molecular rotational levels $J = 2$ are fitted to the experimental data. There is a good agreement between theory and experiment as shown in Fig. 3(b).

4. Conclusion

We have demonstrated an effective approach for enhancing the PA of ultracold atoms using a non-resonant magnetic field. The PA rate coefficient is strongly dependent on the external magnetic field. The enhanced PA can be directly applied to control the atom–molecule conversion. The theoretical calculation based on a simple square-well model, which builds the relationship between the atomic wavefunctions in the interatomic distances $r > \bar{a}$ and $r \leq \bar{a}$, shows a good agreement with the experimental result. Our scheme is helpful to increase the production of ultracold molecules in the PA process. Furthermore, the enhanced PA using non-resonant magnetic fields may provide potential applications to detect the previously unobserved molecular levels due to the small Franck–Condon coupling.

References

[1] Zelevinsky T, Kotochigova S and Ye J 2008 *Phys. Rev. Lett* **100** 043201
[2] Yelin S F, Kirby K and Côté R 2006 *Phys. Rev. A* **74** 050301
[3] Peng X H, Zhang J F, Du J F and Suter D 2009 *Phys. Rev. Lett* **103** 140501
[4] Ospelkaus S, Ni K K, Wang D, de Miranda M H G, Neyenhuis B, Quéméner G, Julienne P S, Bohn J L, Jin D S and Ye J 2010 *Science* **327** 853
[5] Chen P, Li Y Q, Zhang Y C, Wu J Z, Ma J, Xiao L T and Jia S T 2013 *Chin. Phys. B* **22** 093301
[6] Jones K M, Tiesinga E, Lett P D and Julienne P S 2006 *Rev. Mod. Phys* **78** 483
[7] Naidon P and Julienne P S 2006 *Phys. Rev. A* **74** 062713
[8] Zhu S B, Qian J and Wang Y Z 2017 *Chin. Phys. B* **26** 046702
[9] Anderson D A, Miller S A and Raithel G 2014 *Phys. Rev. Lett* **112** 163201
[10] Bohn J L and Julienne P S 1999 *Phys. Rev. A* **60** 414
[11] Kallush S and Kosloff R 2007 *Phys. Rev. A* **76** 053408
[12] Zhang W, Wang G R and Cong S L 2011 *Phys. Rev. A* **83** 045401
[13] Chakraborty D, Hazra J and Deb B 2011 *J. Phys. B: At. Mol. Opt. Phys* **44** 095201
[14] Pellegrini P, Gacesa M and Côté R 2008 *Phys. Rev. Lett* **101** 053201
[15] Tolra B L, Hoang N, T'Jampens B, Vanhaecke N, Drag C, Crubellier A, Comparat D and Pillet P 2003 *Europhys. Lett* **64** 171
[16] Junker M, Dries D, Welford C, Hitchcock J, Chen Y P and Hulet R G 2008 *Phys. Rev. Lett* **101** 060406
[17] Krzyzewski S P, Akin T G, Dizikes J, Morrison Michael A and Abraham E R I 2015 *Phys. Rev. A* **92** 062714
[18] Taie S, Watanabe S, Ichinose T and Takahashi Y 2016 *Phys. Rev. Lett* **116** 043202
[19] Zhao L, Yue D, Liu C, Wang M, Han Y and Gao C 2019 *Chin. Phys. B* **28** 030702
[20] Ren Z M, Wang J and Zhao R X 2019 *Chin. Phys. B* **28** 048301
[21] Kraemer T, Mark M, Waldburger P, Danzl J G, Chin C, Engeser B, Lange A D, Pilch K, Jaakkola A, Nägerl H C and Grimm R 2006 *Nature* **440** 315
[22] Li Y Q, Feng G S, Xu R D, Wang X F, Wu J Z, Chen G, Dai X C, Ma J, Xiao L T and Jia S T 2015 *Phys. Rev. A* **91** 053604
[23] Wang X Q, Li Y Q, Feng G S, Wu J Z, Ma J, Xiao L T and Jia S T 2018 *Chin. Phys. B* **27** 018702
[24] Weber T, Herbig J, Mark M, Nägerl H C and Grimm R 2003 *Science* **299** 232
[25] Wu J Z, Ji Z H, Zhang Y C, Wang L R, Zhao Y T, Ma J, Xiao L T and Jia S T 2011 *Opt. Lett* **36** 2038
[26] Li Y Q, Feng G S, Liu W L, Wu J Z, Ma J, Xiao L T and Jia S T 2015 *Opt. Lett* **40** 2241
[27] McKenzie C, Denschlag J H, Häffner H, Browaeys A, de Araujo Luís E E, Fatemi F K, Jones K M, Simsarian J E, Cho D, Simoni A, Tiesinga E, Julienne P S, Helmerson K, Lett P D, Rolston S L and Phillips W D 2002 *Phys. Rev. Lett* **88** 120403
[28] Lange A D, Pilch K, Prantner A, Ferlaino F, Engeser B, Nägerl H C, Grimm R and Chin C 2009 *Phys. Rev. A* **79** 013622
[29] Bouloufa N, Crubellier A and Dulieu O 2007 *Phys. Rev. A* **75** 052501